

## **Fate of Plutonium at a Former Nuclear Testing Site in Australia**

Ikeda-Ohno, A.; Shahin, L. M.; Howard, D.; Collins, R. N.; Payne, T. E.; Johansen, M. P.;

Originally published:

August 2016

**Environmental Science & Technology 50(2016)17, 9098-9104**

DOI: <https://doi.org/10.1021/acs.est.6b01864>

Perma-Link to Publication Repository of HZDR:

<https://www.hzdr.de/publications/Publ-23556>

Release of the secondary publication  
on the basis of the German Copyright Law § 38 Section 4.

1 The fate of plutonium released from nuclear  
2 weapons tests

3

4 *Atsushi Ikeda-Ohno,<sup>\*,†,‡,§</sup> Lida Mokhber Shahin,<sup>‡</sup> Daryl L. Howard,<sup>□</sup> Richard N. Collins,<sup>§</sup>*  
5 *Timothy E. Payne,<sup>‡</sup> and Mathew P. Johansen,<sup>\*,‡</sup>*

6

7 <sup>†</sup> Helmholtz-Zentrum Dresden-Rossendorf, Institute of Resource Ecology, Bautzner Landstrasse  
8 400, 01328 Dresden, Germany.

9 <sup>‡</sup> Institute for Environmental Research, Australian Nuclear Science and Technology  
10 Organisation, Locked Bag 2001, Kirrawee DC, New South Wales 2232, Australia.

11 <sup>§</sup> School of Civil and Environmental Engineering, the University of New South Wales, Sydney,  
12 New South Wales 2052, Australia.

13 <sup>□</sup> Australian Synchrotron, 800 Blackburn Road, Clayton, Victoria 3168, Australia.

14

15

16 **ABSTRACT**

17 A series of the British nuclear tests conducted on mainland Australia between 1953 and 1963  
18 dispersed long-lived radioactivity and nuclear weapons debris, the legacy of which is a long-  
19 lasting source of radioactive contamination to the surrounding biosphere. A reliable assessment  
20 of the environmental impact of these types of radioactive contaminants and their implications for  
21 human health requires an understanding of their physical/chemical characteristics on the  
22 molecular scale. However, mainly due to the technical difficulties associated with the chemical  
23 diversity of environmental samples, these contaminants have never been characterized  
24 adequately. In this study, we identify the chemical form of plutonium (Pu), one of the most  
25 problematic radionuclides dispersed, in the local soils collected from one of the former weapons  
26 test sites, Maralinga. We herein reveal the first direct spectroscopic evidence that the Pu legacy  
27 exists as particulates of fine Pu oxyhydroxide compounds, a very concentrated and low-soluble  
28 form of Pu, which will serve as ongoing radioactive sources far into the future. We also verify  
29 that the Pu in the particles originated in the so-called “*Minor trials*” that involved the dispersal of  
30 weapon components by highly explosive chemicals, not in the nuclear explosion tests called  
31 “*Major trials*”. The obtained results help us to understand the chemical transformation of the  
32 original Pu materials dispersed in the semi-arid environment more than fifty years ago. These  
33 findings further highlight the importance of the comprehensive physical/chemical  
34 characterization of Pu contaminants for reliable environmental- and radiotoxicological  
35 assessment, which is significantly influenced by the original physical/chemical form of the  
36 contaminant.

37

## 38 INTRODUCTION

39 From 1953 to 1963, the British nuclear weapons testing programme conducted twelve nuclear  
40 detonation tests (“*Major trials*”) and more than five hundred non-nuclear explosion tests (“*Minor*  
41 *trials*”) in the Great Victoria Desert, South Australia (Fig. 1-(a)).<sup>1-2</sup> These tests caused  
42 radioactive contamination with nuclear weapons debris in the test sites and their surroundings.  
43 After completion of official remediation operations in 2002, radionuclides including plutonium  
44 (Pu) remain in activity concentrations that represent extensive environmental contamination with  
45 deposition plumes extending for tens of kilometers outside the clean-up area.<sup>3</sup> A reliable  
46 assessment of the environmental fate of the remaining radioactive contamination and its potential  
47 implication for human health requires detailed knowledge of their chemistry in the relevant  
48 environment; little of which is understood, mainly due to technical difficulties associated with  
49 the analysis of environmental samples with low activity concentrations and complex matrices.<sup>4</sup>  
50 Here we report on a unique analytical approach combining radiochemical analysis with  
51 synchrotron-based X-ray fluorescence microscopy (XFM) to comprehensively characterize the  
52 Pu contaminants resulting from the nuclear weapons tests in Maralinga, Australia (Fig. 1-(a)).

53

54 Figure 1

55

## 56 EXPERIMENTAL

57 **Isolation of Pu-containing particle.** An initial screening of the soil samples to search for the  
58 remaining Pu contaminants was performed by measuring <sup>241</sup>Am activity in the soils with gamma  
59 spectrometry. The presence of <sup>241</sup>Am is largely the result of in-growth following neutron-capture

60 and beta decay reactions from the parent  $^{239}\text{Pu}$ . As a result, the activity concentrations of  $^{241}\text{Am}$   
61 are proportional to those of  $^{239}\text{Pu}$  ( $^{239}\text{Pu}/^{241}\text{Am}$  ratios of 3.4 mean, 0.5 standard deviation) as  
62 measured in the soils of the NW plume. This ratio can vary from plume to plume depending on  
63 the composition of the original tested material.<sup>3,5</sup> Among the collected fifty soil samples, one soil  
64 sample containing the highest  $^{241}\text{Am}$  activity concentration of 1.3 kBq/kg was selected for further  
65 treatment to isolate Pu contaminants. The selected soil sample was then passed through a 125  $\mu\text{m}$   
66 sieve to remove large sand particles and debris. Ten grams of the sieved sample was then  
67 dispersed in 30 ml of lithium heteropolytungstate (LST) heavy liquid ( $D = 2.9$  g/ml) for density  
68 separation. The sample was centrifuged for 5 minutes at 2,000 rpm and the bottom sediments  
69 containing heavy particles were collected. The centrifugation-sediment collection process was  
70 repeated to ensure that the supernatant did not contain heavy particles. The resultant sediments  
71 and supernatant were analysed by gamma spectrometry, which confirmed that the collected  
72 sediments (0.32 g) held at least one particle showing high  $^{241}\text{Am}$  activity. The collected  
73 sediments were further dropped onto the top of a new LST solution to allow the sediments to  
74 stratify only with gentle agitation. Four subsamples were obtained from this stratification  
75 process, only the third densest of which contained almost all of the original  $^{241}\text{Am}$  activity. This  
76 subsample containing  $^{241}\text{Am}$  was further split within small droplets of aqueous solution,  
77 measured by gamma spectrometry, and repeated until a single particle (approximately 150-200  
78  $\mu\text{m}$  in diameter) was identified as a Pu-rich particle. The isolated particle was found to be highly  
79 friable, and, when placed between thin glass slides, easily fragmented into smaller pieces (Fig.  
80 S1 in SI). All fragments exhibited  $^{241}\text{Am}$  activity approximately proportional to their respective  
81 masses, and thus indicated the presence of Pu in similar per mass activity concentrations,  
82 consistent with their origin from a single particle. The isolation process of the Pu particle

83 involved only physical sieving and use of LST solution and deionised water. As the Pu particle  
84 was in a stable chemical form when collected, contact with LST solution (*i.e.*, Li<sup>+</sup> and  
85 polytungstate anions) and deionised water would not cause any further change in the chemical  
86 composition of the particle. Additionally, the employed LST solution was almost saturated ( $D =$   
87 2.9 g/ml, where 2.95 g/ml is the maximum density at 298 K). Hence, the dissolution of other co-  
88 existing minerals/soils during the LST density separation process and subsequent sorption of the  
89 dissolved mineral/soil components on the particle surface is very unlikely. Therefore, the isolated  
90 particle should reflect the current chemical form of Pu at the Taranaki test site.

91 **X-ray fluorescence microscopy and X-ray absorption spectroscopy.** Fragmented pieces of the  
92 isolated particle (five pieces in total) were mounted on a Kapton tape and covered with Ultralene  
93 X-ray fluorescence film (4  $\mu\text{m}$  in thickness) for transport to the Australian Synchrotron. Figure  
94 S3 in the SI shows optical microscope images of the fragments employed for XFM experiments.  
95 XFM measurements were performed at the XFM beamline<sup>6</sup> of the Australian Synchrotron under  
96 ring operating conditions of 3 GeV and 200 mA with top-up mode. Scanning X-ray fluorescence  
97 (XRF) mapping<sup>7</sup> and X-ray absorption near edge structure (XANES) mapping in fluorescence  
98 mode<sup>8</sup> at the Pu L<sub>III</sub>-edge (18.057 keV) were carried out under ambient conditions with a  
99 Kirkpatrick-Baez (KB) mirror pair and the Maia detector.<sup>9</sup> XANES mapping produces a XANES  
100 spectrum from the X-ray fluorescence signal at selected pixels in a stack of images collected as a  
101 function of incident beam energy. For XANES mapping measurements, X-ray absorption spectra  
102 of Zr foil was acquired simultaneously in transmission mode for energy calibration (at the Zr K-  
103 edge, defined as 17999.35 eV at the 1st inflection point) upstream of the KB mirrors. The  
104 acquired data were treated and analysed with the software GeoPIXE (Version 6.6)<sup>10</sup> and  
105 WinXAS (Version 3.2).<sup>11</sup> The acquired X-ray fluorescence data were deconvoluted based on the

106 Dynamic Analysis matrix transform method<sup>12</sup> to obtain elemental concentration maps as a  
107 function of incident beam energy. Pu L<sub>III</sub>-edge X-ray absorption spectra were produced based on  
108 the total counts of the observed Pu L fluorescence lines (Fig. S4 in SI) on a selected region  
109 covering the whole area of each sample fragment. The data treatment for the extended X-ray  
110 absorption fine structure (EXAFS) region was performed with the software WinXAS<sup>11</sup> according  
111 to the standard procedure.<sup>13</sup> Theoretical phase and amplitude for EXAFS theoretical fitting were  
112 calculated by a program code FEFF8.20<sup>14</sup> based on the crystal structures of metallic Pu and  
113 PuO<sub>2</sub>.<sup>15</sup>

114

## 115 **RESULTS AND DISCUSSION**

116 **History of plutonium legacy at the Taranaki test site, Maralinga.** Soil samples were collected  
117 in September 2010 at a distance of 2.0 km from the former firing pad of the Taranaki site, one of  
118 the test sites at Maralinga (Figs. 1-(b) and -(c)). At the Taranaki site, in addition to one “*Major*  
119 *trial*” in 1957, twelve “*Minor trials*” were conducted between 1960 and 1963.<sup>2</sup> These tests  
120 dispersed more than 22 kg of Pu, resulting in four contaminated plumes radiating from the test  
121 site.<sup>2</sup> The sampling point is situated within the northwest (NW) plume (Fig. 1-(c)), where the  
122 main radioactive contamination was caused by the Minor trial “*Vixen B2 – Round 5*” undertaken  
123 in May 1961.<sup>2, 16</sup> The “*Vixen B*” trials involved the burning and detonation of nuclear weapon  
124 components with high-explosives to ascertain the potential for accidents to trigger nuclear  
125 explosions.<sup>2</sup> A “limited number of fissions” during testing were reported,<sup>2</sup> suggesting that the  
126 original Pu materials employed for the trials was presumably metallic Pu with fissile <sup>239,241</sup>Pu

127 isotopes. Hence, the Pu in the soils gathered at the Taranaki site could have originated from  
128 nuclear detonation, limited nuclear fission, or non-nuclear high-explosive dispersal events.

129

130 **Identification of plutonium legacy.** The collected soil samples were first analyzed by gamma  
131 spectrometry and autoradiography to find Pu debris in the soil mixture. After a repetitive process  
132 including sample fractionation, gamma spectrometry and autoradiography, a single particle with  
133 approximately 40 Bq-<sup>241</sup>Am, a major daughter nuclide of <sup>239</sup>Pu, was successfully isolated. The  
134 gamma-ray spectrum of this particle indicated the absence of fission products (FPs) (Fig. S2 in  
135 SI), suggesting that the Pu in the isolated particle did not undergo fission reactions and, hence, it  
136 is likely to originate in “*Minor trials*”, not from “*Major trials*”.

137 Because of the physical/chemical complexity and diversity, the chemical analysis of  
138 environmental samples is always a challenging task.<sup>4</sup> Synchrotron-based XFM is an emerging  
139 and powerful tool to comprehensively characterize not only environmental samples<sup>17</sup> but also  
140 biological and geological samples,<sup>18</sup> providing the information on elemental distribution,  
141 oxidation states and local structural arrangement of the target atoms in a non-destructive manner.  
142 Shown in the upper-left of Fig. 2 is an optical microscope image of one fragment of the isolated  
143 Pu particle. The X-ray fluorescence spectrum of this fragment was found to be primarily  
144 composed of Ca K-, Fe K-, Pb L-, U L- and Pu L-lines (Fig. S4 in SI), suggesting the dominant  
145 presence of these elements in the fragment. No major FPs of Pu isotopes (e.g., noble metals or  
146 lanthanides) were detected, being consistent with the results of gamma spectrometry (Fig. S2 in  
147 SI). The XFM images of the fragment (Fig. 2) further reveal that Pb and Pu are more  
148 concentrated inside the fragment, while Ca, Fe and U are distributed mainly on the outer surface  
149 of the fragment. These elemental distributions, together with the XFM results for other fragments



150 from the same Pu particle (Figs. S5-S10 in SI), point to the fact that the isolated Pu particle  
151 forms the “*core-shell*” structure composed of the Pu+Pb core surrounded by the external shell  
152 containing Ca, Fe and U (Fig. S12 in SI).

153

154 Figure 2

155

156 The chemical state of Pu in the fragment was further investigated by X-ray absorption  
157 spectroscopy. The spectral shape of the fragment in the X-ray absorption near-edge structure  
158 (XANES) region is not consistent with that for Pu-metal,<sup>19</sup> the original Pu compound dispersed at  
159 the site, but rather similar to those for oxide compounds, such as PuO<sub>2</sub> (inset of Fig. 3).<sup>19</sup> The  
160 XANES absorption edge and peak positions of the fragment, both of which are indicative of the  
161 oxidation states and chemical compositions,<sup>20</sup> are comparable with those of Pu(IV) compounds,  
162 such as PuO<sub>2</sub>,<sup>19</sup> or oxyhydroxides<sup>21</sup> (Fig. 3). The extended X-ray absorption fine structure  
163 (EXAFS) spectrum further indicates the presence of Pu□O and Pu□Pu arrangements around the  
164 Pu atoms in the fragment, which is consistent with the structure of oxide or oxyhydroxide  
165 compounds (Fig. S15 and Table S1 in SI). This also excludes the possible presence of  
166 intermetallic Pu compounds in the fragment, such as Pu□Pb compounds.

167

168 Figure 3

169

170 **Transformation of original plutonium materials.** In the “*Vixen B*” trials, the explosions were  
171 reportedly triggered by a high-explosive chemical, such as TNT,<sup>2</sup> which can generate  
172 temperatures over 3,000 °C.<sup>22</sup> The initial Pu component (i.e., metallic Pu) was, therefore, subject  
173 to a high temperature environment during explosion, which prompted the instant oxidation to  
174 PuO<sub>2</sub>, the highest oxidation state and most stable form of Pu oxide compounds.<sup>23</sup> Other lower Pu  
175 oxides, such as Pu<sub>2</sub>O<sub>3</sub>, are unstable and eventually transformed into PuO<sub>2</sub>.<sup>24</sup> The metallic Pu is  
176 also known to be self-ignitable in the air at temperatures exceeding 500 °C, resulting in the  
177 formation of PuO<sub>2</sub>.<sup>25</sup> Based on these facts, it is reasonable to posit that the initial Pu component  
178 was transformed into PuO<sub>2</sub> immediately after the explosion and blasted over the test site as fine  
179 particles, as illustrated in Fig. 4. Subsequently, the scattered PuO<sub>2</sub> particles underwent local  
180 weathering including the interaction with moisture from ambient humidity over more than fifty  
181 years before sampling. PuO<sub>2</sub> is susceptible to moisture even under atmospheric conditions and  
182 eventually transformed into PuO<sub>2+x</sub>,<sup>24</sup> which can be more accurately described as PuO<sub>2+x</sub>.  
183 <sub>y</sub>(OH)<sub>2y</sub>·zH<sub>2</sub>O.<sup>21</sup> The chemical interaction of these Pu compounds with local minerals and soils  
184 could potentially occur via, for instance, the dissolution of Pu into water. However, both PuO<sub>2</sub>  
185 and PuO<sub>2+x</sub>.<sub>y</sub>(OH)<sub>2y</sub>·zH<sub>2</sub>O are expected to be sparingly soluble<sup>26</sup> in the local climate conditions at  
186 Maralinga,<sup>2</sup> suggesting that the chemical form of Pu would be unlikely to be affected by  
187 prolonged exposure to the local minerals and soil environment. Hence, PuO<sub>2+x</sub>.<sub>y</sub>(OH)<sub>2y</sub>·zH<sub>2</sub>O is  
188 likely to be the final form of Pu in the particulate debris remaining at the Taranaki site. This  
189 oxyhydroxide form of Pu shows a characteristic high-energy shift in the XANES peak position  
190 as compared with PuO<sub>2</sub>,<sup>19,21</sup> which is consistent with our XANES data in Figs. 2 and S13 in SI.  
191 The Pu oxyhydroxides could be poorly structured due to the partial oxidation of Pu(IV) to higher  
192 oxidation states.<sup>21,27</sup> This could account for the EXAFS results indicating lower coordination

193 numbers for Pu□O and Pu□Pu shells in the fragments as compared with those in PuO<sub>2</sub> (Table S1  
194 in SI).

195

196 Figure 4

197

198 As shown in Fig. 2, the distribution of Pb coincides with that of Pu. This suggests that Pb is an  
199 intrinsic component of the particle core and not derived from natural accumulation after the  
200 explosion. The gamma-ray spectrum of the fragments confirmed the absence of radioactive Pb  
201 isotopes, indicating that the Pb probably originates either in Pb-metal/alloy tampers<sup>1</sup> which  
202 surrounded the explosive core of the device, or in the shielding/construction materials of the  
203 firing devices<sup>2</sup> blasted with the Pu fuel component. The Ca, Fe and U forming the outer layer of  
204 the Pu particle are likely to originate in the evaporation of moisture containing dissolved  
205 constituents from local soils, which are reported to be rich in these elements,<sup>28</sup> on the surface of  
206 the core particle.

207 **Implication for radioecology.** The low solubility of the Pu(IV) oxyhydroxide/oxide particles  
208 characterized in this study would reduce Pu mobility in abiotic media. However, it does not  
209 prevent its absorption into living organisms. In the mammals inhabiting the studied site, the Pu  
210 was absorbed across biological membranes into muscle, liver and bone, at significant activity  
211 concentrations.<sup>29</sup> As the Pu particles at the site were friable, any fragmentation will increase  
212 potential for uptake by inhalation and lodgement of sub-µm Pu particles deep in the lung.  
213 Clearance of such particles from the organism can be slow, leading to persistent and highly

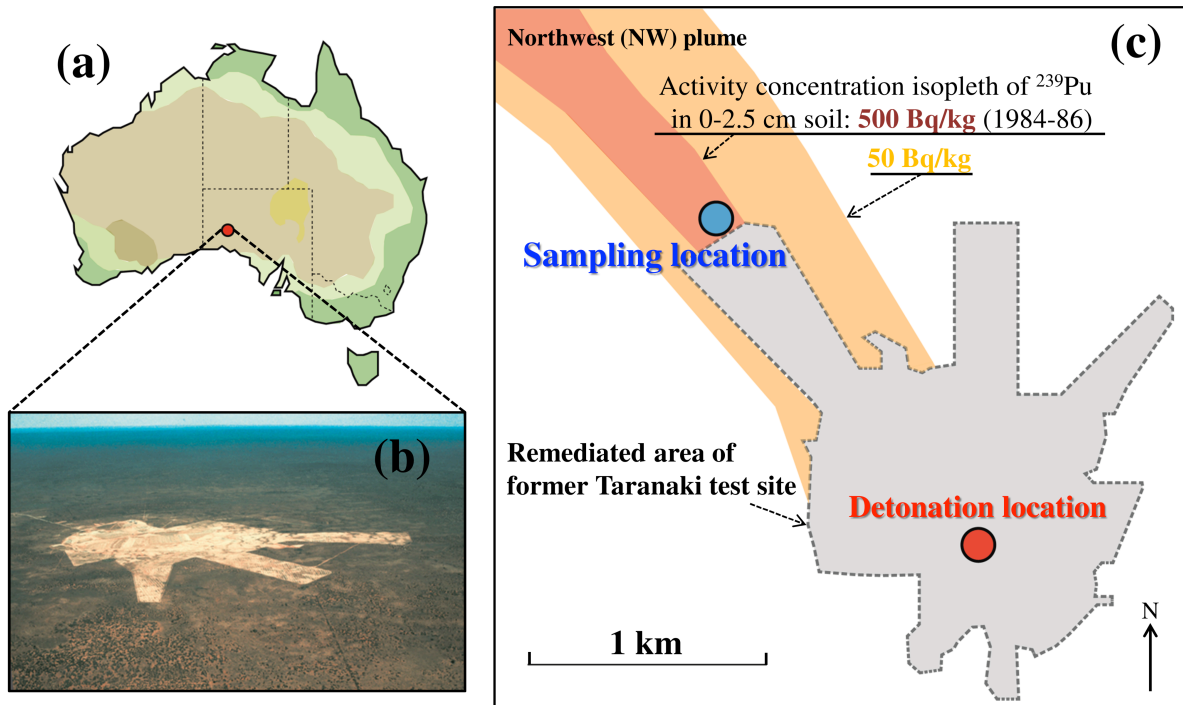
214 concentrated internal Pu sources.<sup>30</sup> This scenario can explain the elevated Pu activity  
215 concentrations observed in some mammals at the Taranaki test site,<sup>29</sup> which could also  
216 potentially occur in case of human uptake. However, the current guidance on radiation safety and  
217 protection<sup>31</sup> is based largely on the uptake of dissolved Pu forms which behave differently from  
218 that of particulates during exposure and uptake. In those cases where particles have been  
219 considered, lung deposition and clearance have been a major concern, with sparse information on  
220 the physical/chemical characteristics of Pu contaminants, due in large part to the difficulty of  
221 evaluating the *in-vivo* behavior of complex Pu particulates.

222 This study provides spectroscopic evidence that the Pu legacy in the particles obtained at the  
223 Taranaki test site originates from unfissioned Pu fuel components, which is a unique source of  
224 Pu contamination as compared not only with those found at most other nuclear test sites, but also  
225 with worldwide fallout, reactor accidents or waste disposal. For instance, the first nuclear test  
226 near Alamogordo, New Mexico, left glassy residues containing fissioned Pu components,<sup>32</sup>  
227 known as “*Trinitite*”, while the Pu legacy from underground nuclear tests at the Nevada Test  
228 Sites (NTS) was associated with mobile colloids facilitating the groundwater transport of  
229 fissioned Pu nuclides.<sup>33</sup> Other non-test-related releases of Pu into the environment include non-  
230 refractory particulates of Pu oxides from non-nuclear accidents.<sup>34</sup> These different forms of Pu  
231 contaminants would behave differently in the environment, resulting in different pathways of  
232 their potential introduction to the human body. With a strong advantage of using synchrotron-  
233 based X-ray microscopy/spectroscopy for the comprehensive characterization of particulate  
234 contaminants, this study highlights the importance of identifying the physical/chemical  
235 characteristics of each Pu contaminant for the reliable assessment of their environmental fate and  
236 potential implication for humans.

237 **FIGURES**

238

239



240

241

242 **Figure 1.** Geographical location of Maralinga (red circle) on an Australian map (a), and an aerial  
243 photo (b)\* and a local map (c) of the Taranaki test site at Maralinga. \*Reprinted with permission  
244 from the Department of Communications, Information Technology and the Arts, the  
245 Commonwealth of Australia (2002).

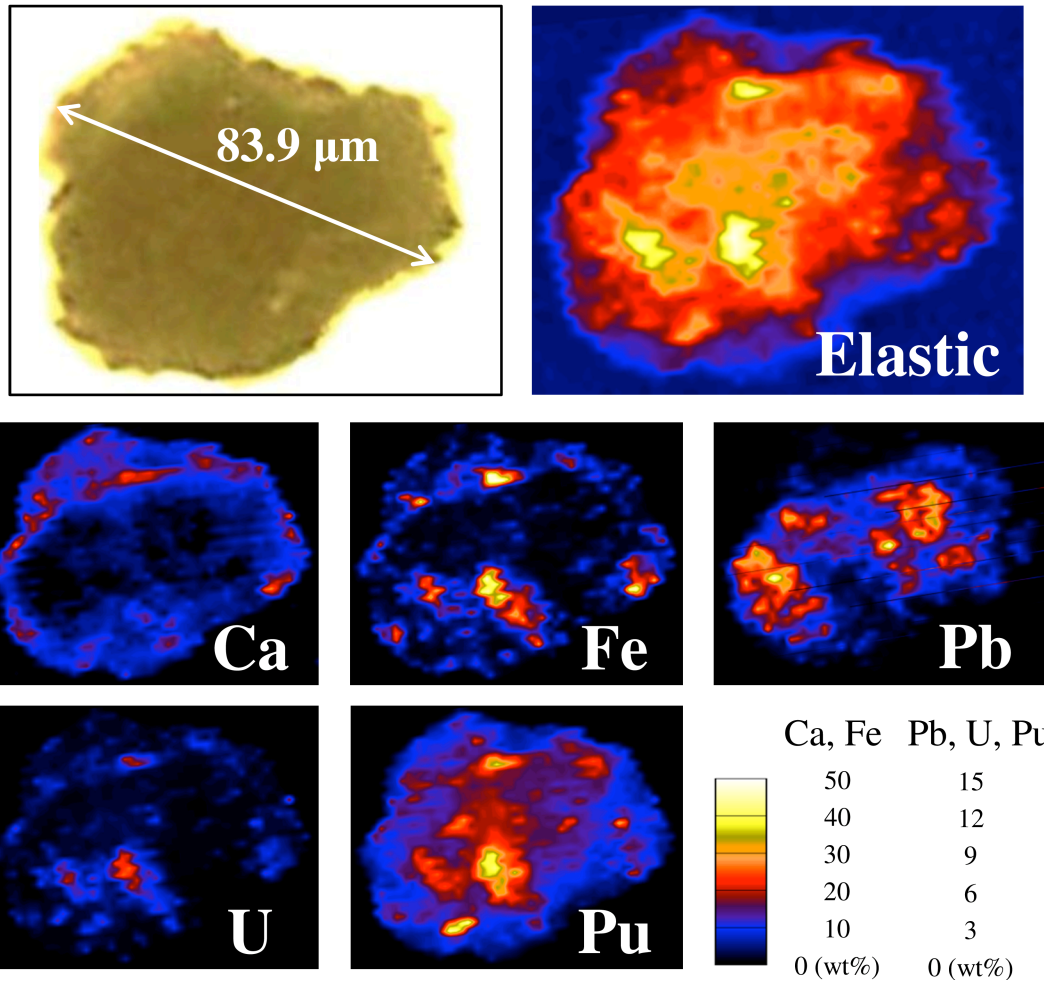
246

247

248

249

250



251

252 **Figure 2.** Optical microscope- (top left) and X-ray fluorescence microscope (XFM) images of a  
253 fragment of the isolated Pu particle deposited at the Taranaki test site.

254

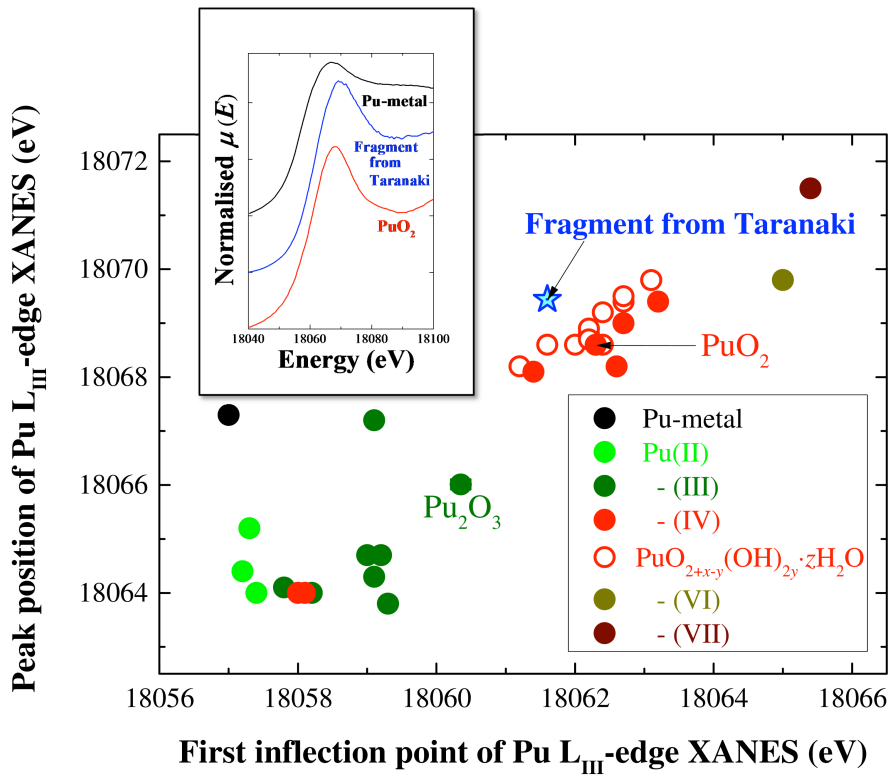
255

256

257

258

259  
260

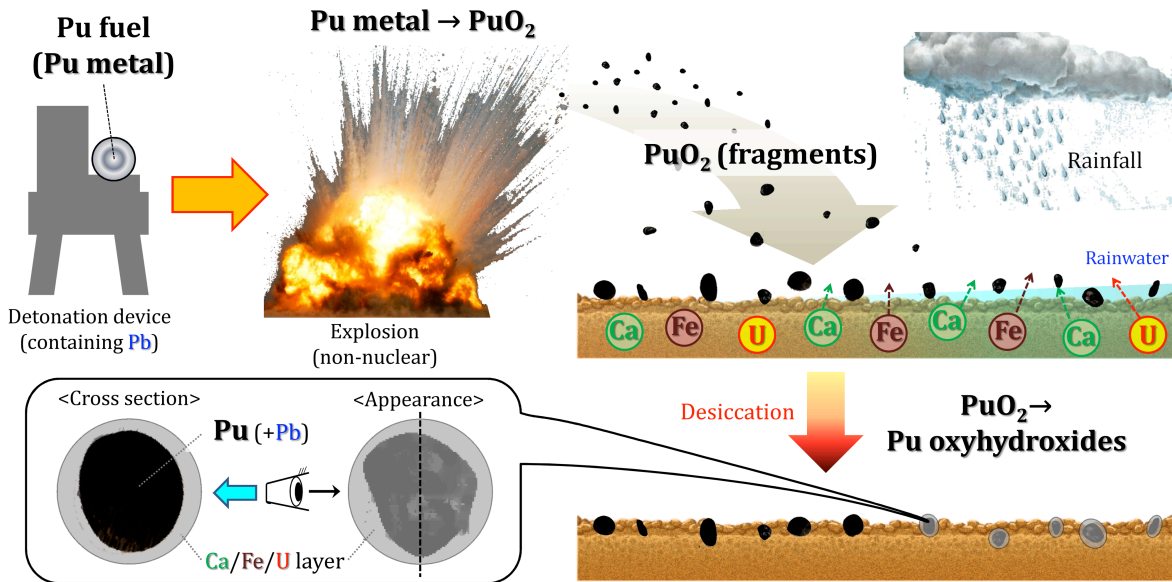


261  
262  
263  
264  
265  
266  
267  
268  
269  
270  
271

**Figure 3.** (Upper inset) Pu L<sub>III</sub>-edge XANES spectra for the fragment of the isolated Pu particle shown in Fig. 2 (blue) and reference compounds of metallic Pu (Pu<sub>0.965</sub>Ga<sub>0.035</sub>, black)<sup>19</sup> and PuO<sub>2</sub> (red).<sup>21</sup> (Main figure) A plot of XANES first inflection points versus their peak positions at Pu L<sub>III</sub>-edge for a series of Pu compounds with different oxidation states. The energy of the data was calibrated according to the first inflection point of Zr foil (defined as 17999.35 eV).

272

273



274

275

276 **Figure 4.** A scenario explaining the possible chemical transformation of Pu weapon components  
277 released in the semi-arid environment by non-nuclear detonation events.

278

279

280

281

282

283

284

285



286 ASSOCIATED CONTENT

287 **Supporting Information.** Gamma spectrum, X-ray fluorescence spectra, X-ray fluorescence  
288 microscopic images and X-ray absorption spectra of the isolated Pu particle, additional  
289 descriptions of experimental details and interpretation of experimental data. This material is  
290 available free of charge via the Internet at <http://pubs.acs.org>.

291

292 AUTHOR INFORMATION

293 **Corresponding Authors**

294 \* E-mail: [a.ikeda@hzdr.de](mailto:a.ikeda@hzdr.de) (A.I.-O.) or [mjo@ansto.gov](mailto:mjo@ansto.gov) (M.P.J.).

295 **Author Contributions**

296 The manuscript was written through contributions of all authors. All authors have given approval  
297 to the final version of the manuscript.

298 **Notes**

299 The authors declare no competing financial interest.

300

301 **ACKNOWLEDGMENT**

302 XFM measurements were performed at the XFM beamline of the Australian Synchrotron,  
303 Victoria, Australia, funded under proposal number 6551. Part of this study was carried out under  
304 the IAEA Coordinated Research Project “Environmental Behaviour and Potential Biological  
305 Impact of Radioactive Particles” (K41013). We also greatly acknowledge Steven D. Conradson

306 (Los Alamos National Laboratory) and Philippe M. Martin (CEA-Cadarache) for providing XAS  
307 data of reference Pu compounds.

308

## 309 REFERENCES

- 310 1. Norris, R. S.; Burrows, A. S.; Fieldhouse, R. W., *British, French, and Chinese nuclear*  
311 *weapons*. Westview Press: 1994; Vol. V.
- 312 2. The Maralinga Rehabilitation Technical Advisory Committee. *Rehabilitation of former*  
313 *nuclear test sites at Emu and Maralinga (Australia) 2003*; 0642-77328-9; The Maralinga  
314 Rehabilitation Technical Advisory Committee: Canberra, Australia, 2003.
- 315 3. Johansen, M. P.; Child, D. P.; Davis, E.; Doering, C.; Harrison, J. J.; Hotchkis, M. A.;  
316 Payne, T. E.; Thiruvoth, S.; Twining, J. R.; Wood, M. D., Plutonium in wildlife and soils  
317 at the Maralinga legacy site: persistence over decadal time scales. *J. Environ. Radioact.*  
318 **2014**, *131*, 72-80.
- 319 4. Fifield, F. W.; Haines, P. J., *Environmental Analytical Chemistry*. 2nd ed.; Wiley-  
320 Blackwell: 2000.
- 321 5. Child, D. P.; Hotchkis, M. A. C., Plutonium and uranium contamination in soils from  
322 former nuclear weapon test sites in Australia. *Nuclear Instruments and Methods in*  
323 *Physics Research Section B: Beam Interactions with Materials and Atoms* **2013**, *294*,  
324 642-646.
- 325 6. Paterson, D.; de Jonge, M. D.; Howard, D. L.; Lewis, W.; McKinlay, J.; Starritt, A.;  
326 Kusel, M.; Ryan, C. G.; Kirkham, R.; Moorhead, G.; Siddons, D. P.; McNulty, I.;  
327 Eyberger, C.; Lai, B., The X-ray Fluorescence Microscopy Beamline at the Australian  
328 Synchrotron. *AIP Conf. Proc.* **2011**, *1365* (219), 219-222.
- 329 7. Howard, D. L.; de Jonge, M. D.; Lau, D.; Hay, D.; Varcoe-Cocks, M.; Ryan, C. G.;  
330 Kirkham, R.; Moorhead, G.; Paterson, D.; Thurrowgood, D., High-definition X-ray  
331 fluorescence elemental mapping of paintings. *Anal. Chem.* **2012**, *84* (7), 3278-3286.
- 332 8. Etschmann, B. E.; Ryan, C. G.; Brugger, J.; Kirkham, R.; Hough, R. M.; Moorhead, G.;  
333 Siddons, D. P.; De Geronimo, G.; Kuczewski, A.; Dunn, P.; Paterson, D.; De Jonge, M.  
334 D.; Howard, D. L.; Davey, P.; Jensen, M., Reduced As components in highly oxidized  
335 environments: Evidence from full spectral XANES imaging using the Maia massively  
336 parallel detector. *Amer. Mineralog.* **2010**, *95* (5-6), 884-887.
- 337 9. Ryan, C. G.; Siddons, D. P.; Kirkham, R.; Li, Z. Y.; de Jonge, M. D.; Paterson, D. J.;  
338 Kuczewski, A.; Howard, D. L.; Dunn, P. A.; Falkenberg, G.; Boesenberg, U.; De  
339 Geronimo, G.; Fisher, L. A.; Halfpenny, A.; Lintern, M. J.; Lombi, E.; Dyl, K. A.;  
340 Jensen, M.; Moorhead, G. F.; Cleverley, J. S.; Hough, R. M.; Godel, B.; Barnes, S. J.;  
341 James, S. A.; Spiers, K. M.; Alfeld, M.; Wellenreuther, G.; Vukmanovic, Z.; Borg, S.,  
342 Maia X-ray fluorescence imaging: Capturing detail in complex natural samples. *J. Phys.:*  
343 *Conf. Ser.* **2014**, *499*, 012002.
- 344 10. Ryan, C. G.; Cousens, D. R.; Sie, S. H.; Griffin, W. L.; Suter, G. F., Quantitative PIXE  
345 microanalysis of geological material using the CSIRO proton microprobe. *Nucl. Inst.*  
346 *Methods Phys. Res. B* **1990**, *47* (1), 55-71.

- 347 11. Ressler, T., WinXAS: a program for X-ray absorption spectroscopy data analysis under  
348 MS-Windows. *J. Synchrotron Radiat.* **1998**, *5* (2), 118-122.
- 349 12. Ryan, C. G., Quantitative trace element imaging using PIXE and the nuclear microprobe.  
350 *Int. J. Imaging Syst. Technol.* **2000**, *11* (4), 219-230.
- 351 13. Prins, R.; Koningsberger, D. E., *X-ray absorption: Principles, applications, techniques*  
352 *for EXAFS, SEXAFS, and XANES*. Wiley Interscience: New York, 1988.
- 353 14. Ankudinov, A. L.; Ravel, B.; Rehr, J. J.; Conradson, S. D., Real-space multiple-scattering  
354 calculation and interpretation of x-ray-absorption near-edge structure. *Phys. Rev. B* **1998**,  
355 *58* (12), 7565-7576.
- 356 15. Wyckoff, R. W. G., *Cryst. Struct.* **1963**, *1*, 7-83, 239-444.
- 357 16. Burns, P. A.; Cooper, M. B.; Johnston, P. N.; Williams, G. A. *Properties of plutonium-*  
358 *contaminated particles resulting from British Vixen B trials at Maralinga*; Australian  
359 Radiation Laboratory: Yallambe, Victoria, Commonwealth of Australia, December 1990,  
360 1990.
- 361 17. Thieme, J.; McNulty, I.; Vogt, S.; Paterson, D., X-ray spectromicroscopy - A tool for  
362 environmental sciences. *Environ. Sci. Technol.* **2007**, *41* (20), 6885-6889.
- 363 18. Lombi, E.; Susini, J., Synchrotron-based techniques for plant and soil science:  
364 opportunities, challenges and future perspectives. *Plant Soil* **2009**, *320* (1-2), 1-35.
- 365 19. Conradson, S. D.; Abney, K. D.; Begg, B. D.; Brady, E. D.; Clark, D. L.; den Auwer, C.;  
366 Ding, M.; Dorhout, P. K.; Espinosa-Faller, F. J.; Gordon, P. L.; Haire, R. G.; Hess, N. J.;  
367 Hess, R. F.; Keogh, D. W.; Lander, G. H.; Lupinetti, A. J.; Morales, L. A.; Neu, M. P.;  
368 Palmer, P. D.; Paviet-Hartmann, P.; Reilly, S. D.; Runde, W. H.; Tait, C. D.; Viers, D. K.;  
369 Wastin, F., Higher order speciation effects on plutonium L<sub>3</sub> X-ray absorption near edge  
370 spectra. *Inorg. Chem.* **2004**, *43* (1), 116-131.
- 371 20. Denecke, M. A., Actinide speciation using X-ray absorption fine structure spectroscopy.  
372 *Coord. Chem. Rev.* **2006**, *250* (7-8), 730-754.
- 373 21. Conradson, S. D.; Begg, B. D.; Clark, D. L.; den Auwer, C.; Ding, M.; Dorhout, P. K.;  
374 Espinosa-Faller, F. J.; Gordon, P. L.; Haire, R. G.; Hess, N. J.; Hess, R. F.; Keogh, D. W.;  
375 Morales, L. A.; Neu, M. P.; Paviet-Hartmann, P.; Runde, W. H.; Tait, C. D.; Viers, D. K.;  
376 Vilella, P. M., Local and nanoscale structure and speciation in the PuO<sub>2+x-y</sub>(OH)<sub>2y</sub>·zH<sub>2</sub>O  
377 system. *J. Am. Chem. Soc.* **2004**, *126* (41), 13443-13458.
- 378 22. Danilenko, V. V., Nanocarbon phase diagram and conditions for detonation nanodiamond  
379 formation. In *Synthesis, Properties and Applications of Ultrananocrystalline Diamond -*  
380 *NATO Science Series II*, Gruen, D. M.; Shenderova, O. A.; Ya. Vul', A., Eds. Springer:  
381 Dordrecht, The Netherland, 2005; Vol. 192, pp 181-198.
- 382 23. Clark, D. L.; Hecker, S. S.; Jarvinen, G. D.; Neu, M. P., Plutonium. In *The Chemistry of*  
383 *the Actinide and Transactinide Elements*, Third edition ed.; Morss, L. R.; Edelstein, N.  
384 M.; Fuger, J.; Katz, J. J., Eds. Springer: Dordrecht, The Netherland, 2006; Vol. 2.
- 385 24. Haschke, J. M.; Allen, T. H.; Morales, L. A., Surface and corrosion chemistry of  
386 plutonium. *Los Alamos Science* **2000**, *26*, 252-273.
- 387 25. Martz, J. C.; Haschke, J. M.; Stakebake, J. L., A mechanism for plutonium pyrophoricity.  
388 *J. Nucl. Mater.* **1994**, *210* (1-2), 130-142.
- 389 26. Neck, V.; Altmaier, M.; Seibert, A.; Yun, J. I.; Marquardt, C. M.; Fanghänel, T.,  
390 Solubility and redox reactions of Pu(IV) hydrous oxide: Evidence for the formation of  
391 PuO<sub>2+x</sub>(s, hyd). *Radiochim. Acta* **2007**, *95* (4), 193-207.

- 392 27. Haschke, J. M.; Allen, T. H.; Morales, L. A., Reaction of plutonium dioxide with water:  
393 Formation and properties of  $\text{PuO}_{2+x}$ . *Science* **2000**, 287 (5451), 285-287.
- 394 28. Cooper, M. B.; Burns, P. A.; Tracy, B. L.; Wilks, M. J.; Williams, G. A., Characterization  
395 of plutonium contamination at the former nuclear weapons testing range at Maralinga in  
396 South Australia. *J. Radioanal. Nucl. Chem.* **1994**, 177 (1), 161-184.
- 397 29. Johansen, M. P.; Child, D. P.; Caffrey, E. A.; Davis, E.; Harrison, J. J.; Hotchkis, M. A.  
398 C.; Payne, T. E.; Ikeda-Ohno, A.; Thiruvoth, S.; Twining, J. R.; Beresford, N. A.,  
399 Accumulation of plutonium in mammalian wildlife tissues following dispersal by  
400 accidental-release tests. *J. Environ. Radioactiv.* **2016**, 151 (2), 387-394.
- 401 30. ICRP *Human respiratory tract model for radiological protection*. ICRP Publication 66,  
402 *Ann. ICRP* 24 (1-3); International Commission on Radiological Protection: 1994.
- 403 31. ICRP *Compendium of dose coefficients based on ICRP Publication 60*, ICRP Publication  
404 119, *Ann. ICRP* 41(2); International Commission on Radiological Protection: 2012.
- 405 32. Fahey, A. J.; Zeissler, C. J.; Newbury, D. E.; Davis, J.; Lindstrom, R. M., Postdetonation  
406 nuclear debris for attribution. *Proc. Nat. Acad. Sci. U.S.A.* **2010**, 107 (47), 20207-20212.
- 407 33. Kersting, A. B.; Efurud, D. W.; Finnegan, D. L.; Rokop, D. J.; Smith, D. K.; Thompson, J.  
408 L., Migration of plutonium in ground water at the Nevada Test Site. *Nature* **1999**, 397  
409 (6714), 56-59.
- 410 34. Donohue, D. L., Strengthened Nuclear Safeguards. *Anal. Chem.* **2002**, 74 (1), 28A-35A.

411

412

413

414

415

416

417

418

419

420

421 **Table of Contents Graphic and Synopsis**



422

423 The plutonium legacy from a former nuclear weapons test in Australia was characterized as a  
424 particulate form of Pu(IV) oxyhydroxides, which would be a potential source of long-term  
425 internal radiation if lodged within an organism.

426

427